

Signal-noise separation using unsupervised reservoir computing

Jaesung Choi¹ and Pilwon Kim*²

¹*Center for Artificial Intelligence and Natural Sciences, Korea Institute for Advanced Study, Seoul 02455, South Korea*

²*Department of Mathematical Sciences, Ulsan National Institute of Science and Technology, Ulsan 44919, South Korea*

(Dated: 31 May 2024)

Removing noise from a signal without knowing the characteristics of the noise is a challenging task. This paper introduces a signal-noise separation method based on time series prediction. We use Reservoir Computing (RC) to extract the maximum portion of “predictable information” from a given signal. Reproducing the deterministic component of the signal using RC, we estimate the noise distribution from the difference between the original signal and reconstructed one. The method is based on a machine learning approach and requires no prior knowledge of either the deterministic signal or the noise distribution. It provides a way to identify additivity/multiplicativity of noise and to estimate the signal-to-noise ratio (SNR) indirectly. The method works successfully for combinations of various signal and noise, including chaotic signal and highly oscillating sinusoidal signal which are corrupted by non-Gaussian additive/multiplicative noise. The separation performances are robust and notably outstanding for signals with strong noise, even for those with negative SNR.

Keywords: denoising, data filtering, time series data, reservoir computing, echo state network

I. INTRODUCTION

Recovering the signal using data contaminated by noise is a long-standing challenge in signal and image processing¹⁻⁴. Estimation of the noise distribution is a key factor in determining the effectiveness of noise removal algorithms. In general, such algorithms are designed to work well for a specific distribution of noise. For example, algorithms that are designed to remove Gaussian noise will not perform as well for non-Gaussian noise. When handling denoising without prior knowledge of the noise distribution, it is often necessary to try a variety of algorithms such as low-pass filtering, wavelet-based smoothing and nonlinear adaptive filtering, and see which one works best^{5,6}. However, those trials may not be able to remove the noise effectively and often introduce artifacts to the recovered signal.

The signal-noise separation task becomes even more challenging if there is no reliable noise model. As the methods for dealing with multiplicative noise significantly differ from those employed for additive noise. Identifying whether the signal is corrupted by additive noise, multiplicative noise, or a combination of both is crucial for accurate signal analysis^{7,8}.

In this paper we consider the separation of signal from data contaminated by noise with unknown structure. More precisely, no assumption is made on the noise model or the noise distribution, and the separation is solved based only on the corrupted signal observations. The method proposed in this paper is based on time series prediction. Due to recent advances in machine learning, various time series analysis techniques have been proposed, including methods based on neural networks, and it is now possible to find deterministic patterns effectively even in a single time series. This allows us to redefine the signal filtering problem as a signal reconstruction problem.

Treating a given signal as training data, we instruct the machine predictor to discover as much predictable patterns within the signal as possible. If the predictor is not biased

and its capacity is properly optimized within a range not to overfit data, the predictor can extract the deterministic portion of the signal successfully. By comparing the signal reconstructed through this process to the original one, we can identify whether the noise is additive or multiplicative, and can effectively approximate the target signal and the noise distribution together.

The proposed method was tested on several types of signal and noise. We focused on the separation of seemingly noise-like target signals under various non-Gaussian noises: this includes discrete/continuous chaotic signal with additive multimodal noise and highly oscillating signal with multiplicative gamma noise.

The paper is organized as follows. In the next section we formulate the separation problem. Section III explains the core procedures of the signal-noise separation. We deal with a reservoir computing method in Section IV which serves as a time series predictor in this paper. In Section V, by applying the preceding procedures, we identify whether the noise is additive or multiplicative, and then obtain its distribution accordingly. Section VI deals with validation to optimize the hyperparameters of the predictor. In Section VII, the proposed method is applied to combinations of various signal and noise. The results are compared to those from conventional filters.

II. PROBLEM FORMULATION

Let $x_i; i = 0, 1, \dots, N$ be the signal of interest for noise separation. We assume the signal follows either the observational model for additive noise

$$x_i = q_i + \xi_i, \quad E[\xi_i] = 0, \quad (1)$$

or the model for multiplicative noise

$$x_i = q_i \xi_i, \quad E[\xi_i] = 1. \quad (2)$$

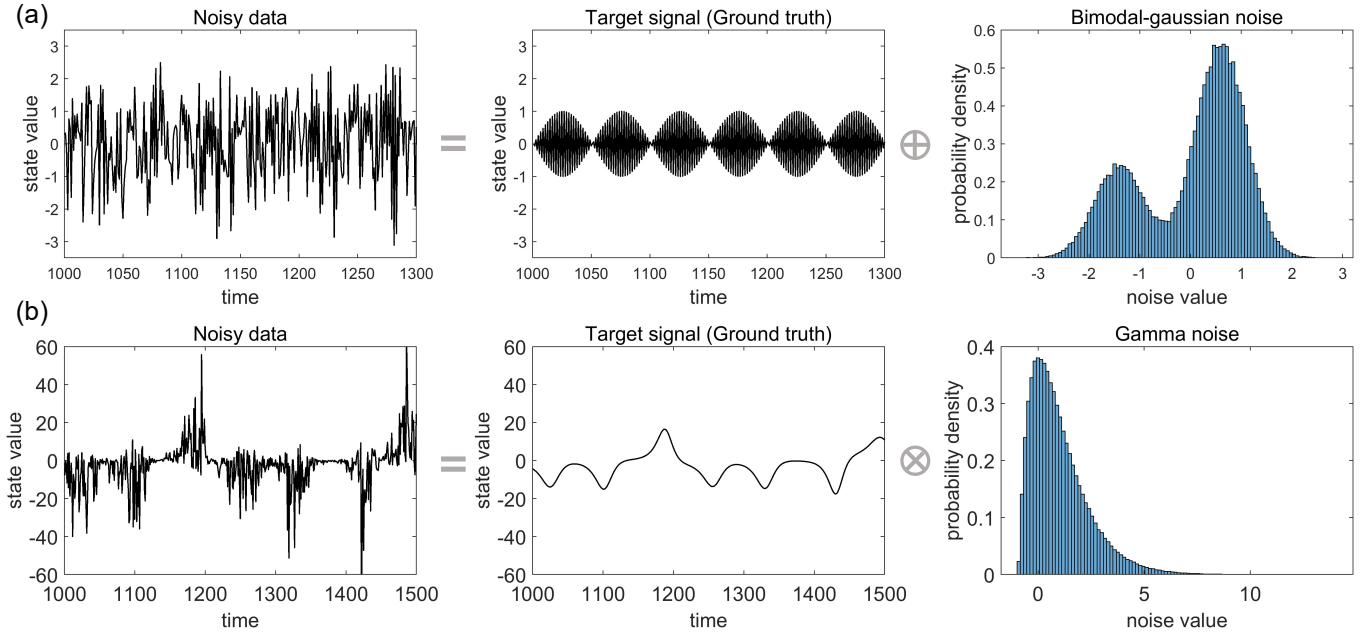


FIG. 1: signal-noise separation for (a) additive noise and (b) multiplicative noise

Here q_i is the deterministic signal component and ξ_i is the noise component at the i th sampling instant. We assume no prior knowledge on the deterministic mechanism for q_i nor on the noise distribution for ξ_i .

By comparing the given signal x_i with the signal q_i reconstructed from a machine learning method, we characterize the form of noise ξ_i either as (1) or (2), and then estimate its distribution accordingly.

Figure 1 illustrates two examples of separation of the signal: (a) highly oscillating sinusoidal signal with additive bimodal-gaussian noise and (b) chaotic signal with multiplicative gamma noise. This separation procedure will be handled in detail in the following sections.

III. OUTLINE OF THE SEPARATION PROCEDURE

We treat the given signal $x_i, 0 \leq i \leq N$ to be processed as a dataset for learning, and split it into a training part $x_i, 0 \leq i \leq K$ and a validation part $x_i, K < i \leq N$. We adopt a m -step time series predictor P based on a machine learning method which supposedly reproduces one step ahead from previous steps as $x_i = P(x_{i-1}, x_{i-2}, \dots, x_{i-m}), m \leq i \leq N$ after learning the signal.

The signal-noise separation for $x_i, m \leq i \leq N$ with respect to P proceeds in the following six steps.

1. Training the predictor P to minimize the cost function over the training part,

$$\sum_{i=m}^K \|x_i - P(x_{i-1}, x_{i-2}, \dots, x_{i-m})\|^2.$$

2. Reconstruction of q_i using the predictor P :

$$\hat{q}_i = P(x_{i-1}, x_{i-2}, \dots, x_{i-m}), \quad m \leq i \leq N.$$

3. Evaluation of misfits :

$$\psi_i = x_i - P(x_{i-1}, x_{i-2}, \dots, x_{i-m}) = x_i - \hat{q}_i, \quad m \leq i \leq K.$$

4. Identification of additivity/multiplicativity of noise from the correlation between ψ_i and \hat{q}_i

5. Approximation of the noise distribution D :

$$\hat{\xi}_i = \psi_i, \quad \text{for } m \leq i \leq K.$$

(or $\hat{\xi}_i = \psi_i / \hat{q}_i$, in case of multiplicative noise)

6. Evaluation of the approximate error over the validation part:

$$\sum_{i=m}^K \|x_i - \hat{q}_i\|^2.$$

Note that the time series predictor P is not actually used to predict $x_i, i > N$, but rather to reconstruct the original time series $x_i, m \leq i \leq N$. Considering the deterministic nature of pattern prediction, we expect that the training process “neutralizes” the effect of noise ξ_i and yields estimation of the deterministic portion q_i .

Step 6 is necessary to optimize the hyperparameters of the predictor P . We repeat Step 1 through 6 using a hyperparameter-tuning method such as Bayesian optimization, until the validation error reaches its minimum. The validation process will be discussed in more detail in Section VI.

IV. RESERVOIR COMPUTING PREDICTOR

The predictor P in the process outlined in the previous section can be implemented with any common machine learning methods. Reservoir computing (RC) is one of the popular choices to deal with time series due to its simple architecture and dynamic nature⁹. RC comprises two main components: (i) a “reservoir” is a fixed nonlinear recurrent network and (ii) a “readout” is a trainable linear output layer.

We especially use a simple discrete type of RC, Echo State Networks (ESN) to predict the time series $x_i, i = 0, 1, \dots$. ESN consists of L nodes whose temporal states $\mathbf{r}(i) \in \mathbb{R}^L$ evolves through the equation:

$$\mathbf{r}(i+1) = (1-\alpha)\mathbf{r}(i) + \alpha \tanh(\mathbf{A}\mathbf{r}(i) + \mathbf{W}_{\text{in}}x_{i-1}), i = 1, 2, \dots, \quad (3)$$

where α is a leaking rate, $\mathbf{A} \in \mathbb{R}^{L \times L}$ the internal weight matrix, and $\mathbf{W}_{\text{in}} \in \mathbb{R}^L$ the input weight vector. For more general introduction to ESN, the readers are referred to^{10,11}. The readout weight vector \mathbf{W}_{out} is determined in the training process by solving:

$$\mathbf{W}_{\text{out}} = \arg \min_{\mathbf{W} \in \mathbb{R}^N} \left(\sum_{i=1}^K \|x_{i+1} - \mathbf{W}^T \mathbf{r}(i)\|^2 + \lambda \|\mathbf{W}\|_F^2 \right), \quad (4)$$

where λ is a regularization parameter.

Once \mathbf{W}_{out} is obtained, we can estimate the deterministic signal as

$$\hat{q}_i = \mathbf{W}_{\text{out}} \mathbf{r}(i), i = 0, 1, \dots, N. \quad (5)$$

to implement the separation process described in Section 3. We call this Signal-Separation using Reservoir Computing (SSRC).

V. IDENTIFICATION OF ADDITIVITY /MULTIPLICATIVITY OF NOISE

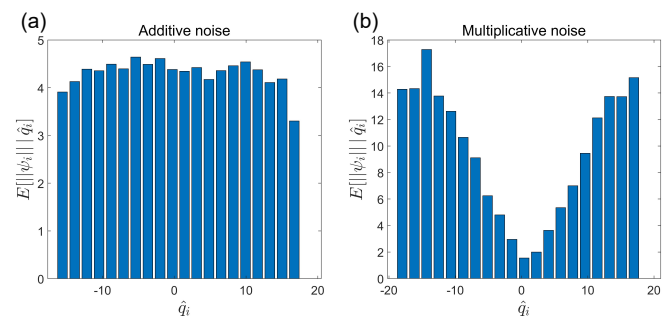


FIG. 2: Graphs of $E[||\psi_i|| | \hat{q}_i]$ with respect to \hat{q}_i : (a) additive noise (b) multiplicative noise.

We can discriminate between additive and multiplicative noise, by studying the conditional distribution of the misfit ψ_i , given \hat{q}_i . More specifically, the type of noise can be

inferred from the graph of $E[||\psi_i|| | \hat{q}_i]$ with respect to \hat{q}_i . We use the approximation $E[||\psi_i|| | \hat{q}_i] = E[||x_i - \hat{q}_i|| | \hat{q}_i] \approx E[||x_i - q_i|| | \hat{q}_i]$. In case of additive noise as in Eq. (1), we have

$$E[||x_i - q_i|| | q_i] = E[||\xi_i|| | q_i] = E[||\xi_i||] = \text{const.},$$

since noise ξ_i is independent from the deterministic signal q_i . This leads to a flat graph as in Figure 2(a). On the contrary, multiplicative noise ξ_i in Eq. (2) gives

$$\begin{aligned} E[||x_i - q_i|| | q_i] &= E[||q_i|| | \xi_i - 1 | | q_i] \\ &= ||q_i|| E[||\xi_i - 1||] \approx C ||q_i||, \end{aligned}$$

where $C = E[||\xi_i - 1||] = \text{const.}$ Figure 2(b) shows an example of the corresponding symmetric V-shaped graph with a vertex at the origin.

Once confirmed as additive noise, the approximate noise $\hat{\xi}_i$ and its distribution can be obtained by $\hat{\xi}_i = \psi_i$. In case of multiplicative noise, we set $\hat{\xi}_i = x_i / \hat{q}_i$.

VI. VALIDATION TO AVOID OVERFITTING

The goal of training a predictor P for a given signal x_i is to set P to discover the maximum deterministic patterns, that is, q_i . In Section VII, we will see through a number of examples that the reservoir-based predictor of reasonable size can successfully extract q_i , separating it from various noise. However, P is commonly exposed to risk of overfitting, since it uses only the single signal for training, the very signal that is the subject of the separation. If P has excessive computational capacity, it is likely to overfit in estimating q_i , futilely looking for spurious patterns in the noise.

Such overfitting may arise especially when the deterministic portion of the signal is small compared to noise, that is, when the signal-to-noise ratio (SNR) is small. In other words, at low SNRs, the use of overly powerful predictors can lead to overfitting, which degrades the reliability of the reconstructed signal.

Figure 3(a) is a heat map of the approximation error $||\hat{q}_i - q_i||$ showing this trend. The x-axis represents the number of nodes used for RC, and the y-axis corresponds to the noise level of ξ_i , which linearly determines the standard deviation of ξ_i .

One can determine the optimal number of nodes at a noise level, by comparing the error values along the corresponding horizontal line across the heat map. In Figure 3(b), such three exemplary cross sectional graphs are plotted at the noise level 0.14, 0.38 and 0.9, respectively. All the cross sectional graphs are vertically shifted for the minimum to be placed at zero for convenience of comparison. This shows the optimal choice for the node numbers are 260, 140 and 70, respectively.

The red dotted line in Figure 3(a) indicates where the optimal choice for the reservoir size (node numbers) occurs at each level of the noise. Since the number nodes used in the reservoir roughly indicates its computational capacity, the optimal node number tends to decrease as the noise level in-

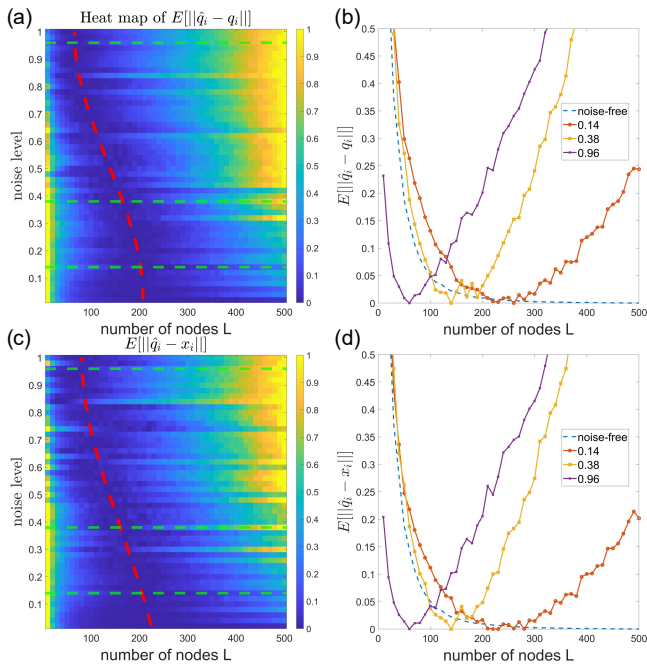


FIG. 3: (Color online) Optimal reservoir size according to the noise level. (a) Heat map of $E[||\hat{q}_i - q_i||]$ with respect to the reservoir size and the noise level (b) Horizontal cross sectional graphs of (a) at the noise level 0.14, 0.38 and 0.96 (13.92, 5.28 and -2.9dB in SNR, respectively). (c) Heat map of $E[||\hat{x}_i - x_i||]$ with respect to the reservoir size and the noise level (d) Horizontal cross sectional graphs of (c) at the noise level 0.14, 0.38 and 0.96. The red dotted lines in (a) and (c) indicate the optimal node numbers at each noise level. For convenience of comparison, the heat maps are normalized in a way that the minimum on each horizontal cross sectional line is placed at zero.

creases.

Note that the such optimal choice in Figure 3(a) and (b) was actually determined by comparing the approximate deterministic component \hat{q}_i to the true one q_i . However, q_i is not available in practice. Thus we use the error between the given signal x_i and the reproduced signal \hat{q}_i over the validation set instead. Figure 3(c) and (d) shows that the validation error between \hat{q}_i and x_i largely follows the tendency of the errors between \hat{q}_i and q_i , and therefore is capable to provide the criterion to tune the hyperparameters of the predictor. Refer to the supplement for more detail of the other parameter values used for the figures.

VII. EXPERIMENTS

This section applies the separation procedure described in Section III to various type of signals. We are especially interested in chaotic and highly oscillating target signal q_i , which is often hard to identify from noise. More specifically, three deterministic signals are sampled from (a) Lorenz systems

(b) high-frequency sinusoidal signal and (c) logistic map with memory (mLogistic). Refer to Supplement for more details of the signals including the generating equations.

We test combinations of these signals with the three types of non-Gaussian noise: (1) additive lognormal noise, (2) additive bimodal noise, and (3) multiplicative gamma noise. In all examples, the time series consists of 9000 data points. We allocate 1000 points of them to the validation set and use Bayesian search to determine hyperparameters such as the number of nodes L and the spectral radius of the connection matrix \mathbf{A} .

We compare the separation results with those of conventional methods such as low-pass filters, wavelet filters, median filter and nonlinear adaptive filter. In nonlinear adaptive filtering method outlined by Gao et al.¹², time series is segmented into subintervals and adaptively merged after polynomial fitting for enhanced signal clarity. For these filters, the noise distributions are obtained in a similar manner to the proposed method, that is, from the observation on difference between the original signal and the filtered signal. More detailed information about the filters used for comparison can be found in Supplement. The root-mean square error (RMSE) is used to evaluate the reconstruction error for q_i . To measure how close the distributions of $\hat{\xi}_i$ is to that of ξ_i , we use the Jensen-Shannon divergence (JSD).

A. Signals with additive lognormal noise

In the first set of examples, we test SSRC for signals corrupted by additive lognormal noise. Figure 4 shows a one of the separation results for the signal x_i sampled from the Lorenz system. It is corrupted by additive noise in a one-sided lognormal distribution with SNR is 2.67dB. In Figure 4(a), the reconstructed signal \hat{q}_i by SSRC is plotted. Figure 4(b) is the separation results of the low pass filter whose cut off frequency is the lowest 25% of the spectrum, and 4(c) is those of the wavelet filter (Daubechies-4). It is confirmed that SSRC performs better than the other two methods both in reconstruction of the deterministic and noise component.

Table 1 contains thorough results from the various combinations for the lognormal noise. The second and third rows show the separation performances for the highly oscillating signal and the logistic map with memory, respectively, both of which are corrupted by lognormal noise. In all three cases, we can see that SSRC outperforms the other filter methods in reconstruction of the deterministic signal.

Figure 5 compares the separation performances according to the noise level. Figure 5(a), (b) and (c) shows errors in separation of three types of signals, respectively, corrupted by additive lognormal noise with different levels of SNR. In all bins of the comparison, SSRC outperforms the other filters. We can see that the accuracy in recovering the deterministic component increases as SNR increases. It is notable that the performance of SSRC is almost insensitive to SNR, i.e., it is less affected by the noise level in separation of signals. This forms a striking difference from other filters which have substantial difficulty distinguishing between signal and noise, especially when SNR is small.

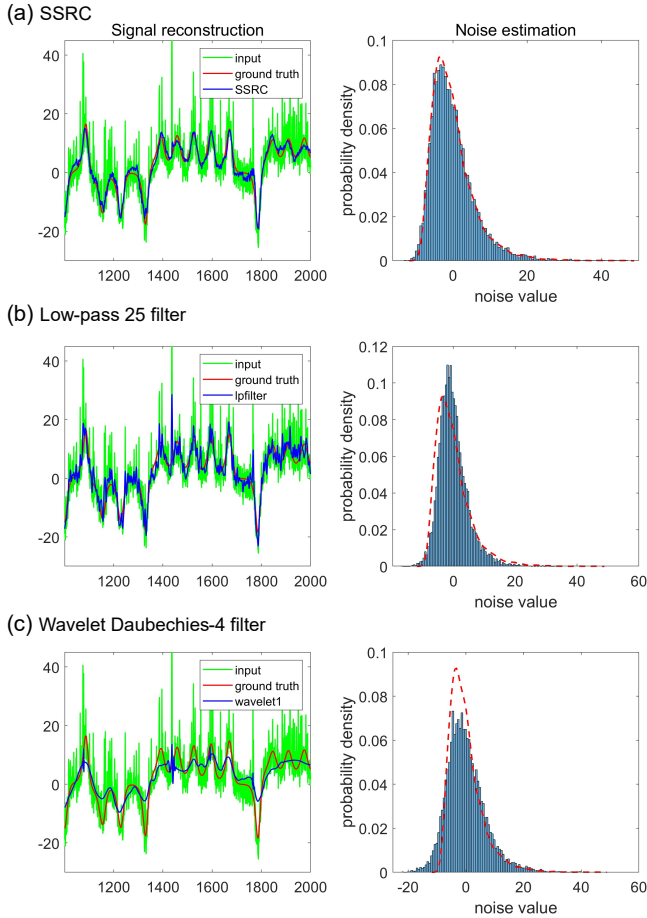


FIG. 4: (Color online) Lorenz signal x_i corrupted by additive lognormal noise with SNR=2.67(dB), (a) separation results of SSRC, (b) low pass filtering, (c) wavelet based filtering

B. Signals with additive multimodal noise

Multimodal noise often arises when measurement systems integrate input from several sources. In the second set of examples, we test SSRC for signals corrupted by multimodal noise. Fig 6 shows one of the separation results. The original signal is a highly oscillating sinusoidal signals corrupted by additive bimodal noise with 4.58(dB). It is clear that the reconstruction by SSRC in Figure 6(a) excels those by the low pass filter and the wavelet filter in Figures 6(b) and 6(c), respectively. Neither of two filters can reproduce a simple deterministic sinusoidal pattern with high frequency. In addition, SSRC successfully captures bimodality of the noise distribution, while the others fail to detect it.

Table 2 also confirms the separation performance of SSRC is better than the other conventional filters in three types of signals corrupted by the bimodal noise. Figure 7 compares the performance of methods according to SNR. Once again, SSRC turned out to be better than the other filters in all bins of the comparison.

	Lorenz	High frequency	mLogistic
SSRC	0.1786	0.0452	0.0661
Wavelet1	0.4865	1.0001	0.3789
Wavelet2	0.4871	1.0001	0.3750
Low-pass Filtering25	0.3349	1.0031	0.2738
Low-pass Filtering50	0.4786	1.0063	0.1712
Low-pass Filtering75	0.6039	1.0099	0.1278
Median Filtering	0.3624	0.2216	0.2659
Adaptive filtering	0.1994	1.0007	0.3784

TABLE I: Mean reconstruction errors for additive log-normal noise with various data types of average SNR values of 2.67 dB, 15.3 dB, and 21.6 dB for Lorenz, high-frequency, and mLogistic system, respectively, out of 100 realizations.

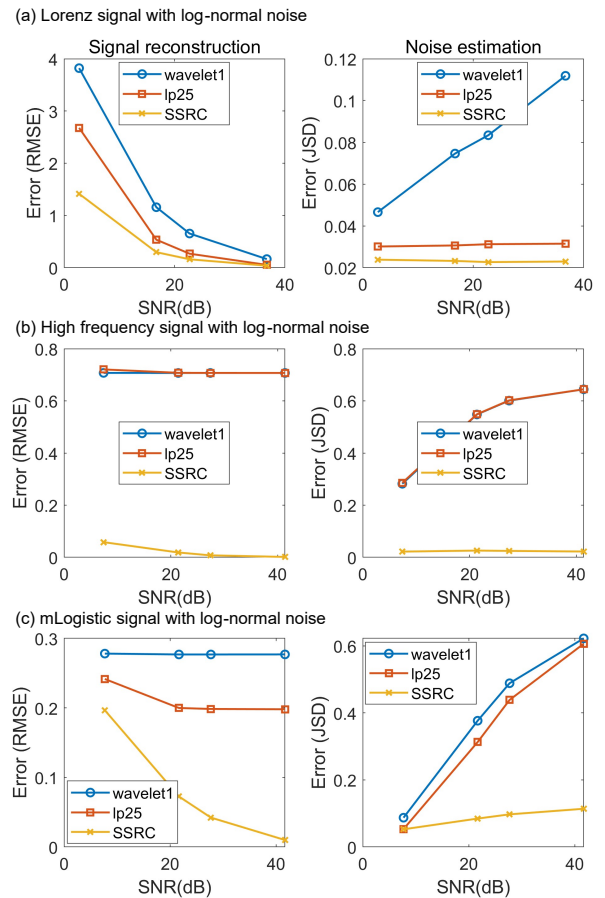


FIG. 5: Comparison of separation performance for additive log-normal noise according to SNR. (a) Lorenz signal (b) Highly oscillating sinusoidal signals

C. Signals with multiplicative gamma noise

Multiplicative noise has been observed in many signal processing applications, biological movement systems and optical systems^{13–16}. Removal of multiplicative noise is challenging because it distorts the amplitude of a signal substantially.

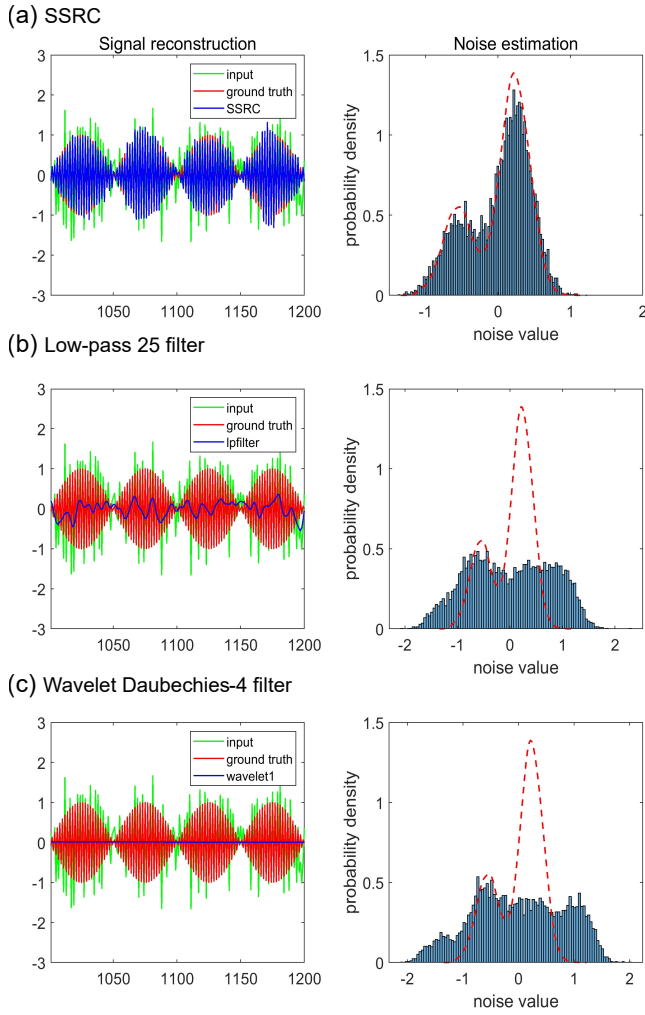


FIG. 6: (Color online) Highly oscillating sinusoidal signals x_i corrupted by additive bimodal-gaussian noise with SNR=4.58(dB), (a) separation results of SSRC, (b) low pass filtering, (c) wavelet based filtering

In the third set of examples, we apply SSRC to signals corrupted by multiplicative noise. Figure 8 shows one of the separation results for a signal from the logistic map with memory. The signal is corrupted by the multiplicative noise with 9(dB) that follows a gamma distribution with mean 1. Figure 8(a), (b) and (c) compare the reconstructed signals \hat{q}_i and the distribution of the error $\hat{\xi}_i$ by SSRC, the low pass filter and the wavelet filter, respectively. Note that the results of SSRC in the plots (a) accompany with verification of the multiplicativity of the noise through the graph in Figure 2(b). On the contrary, one can find no clue about the noise type in processing the other filters. It is clear again that SSRC outperforms two other filters in separating q_i and ξ_i . Refer to Table 3 and Figure 9 for further comparison for other signal-noise combinations at various noise levels.

	Lorenz	High frequency	mLogistic
SSRC	0.4811	0.1578	0.3136
Wavelet1	0.8749	1.0008	0.3809
Wavelet2	0.8708	1.0006	0.3804
Low-pass Filtering25	1.1563	1.0359	0.3768
Low-pass Filtering50	1.6529	1.0722	0.4075
Low-pass Filtering75	2.0871	1.1127	0.4843
Median Filtering	1.5841	0.6020	0.4497
Adaptive filtering	0.5221	1.0070	0.3952

TABLE II: Mean reconstruction errors for additive bimodal-gaussian noise with various data types of SNR values of -8.01 dB, 4.58 dB, and 5.1 dB for Lorenz, high-frequency, and mLogistic system, respectively, out of 100 realizations.

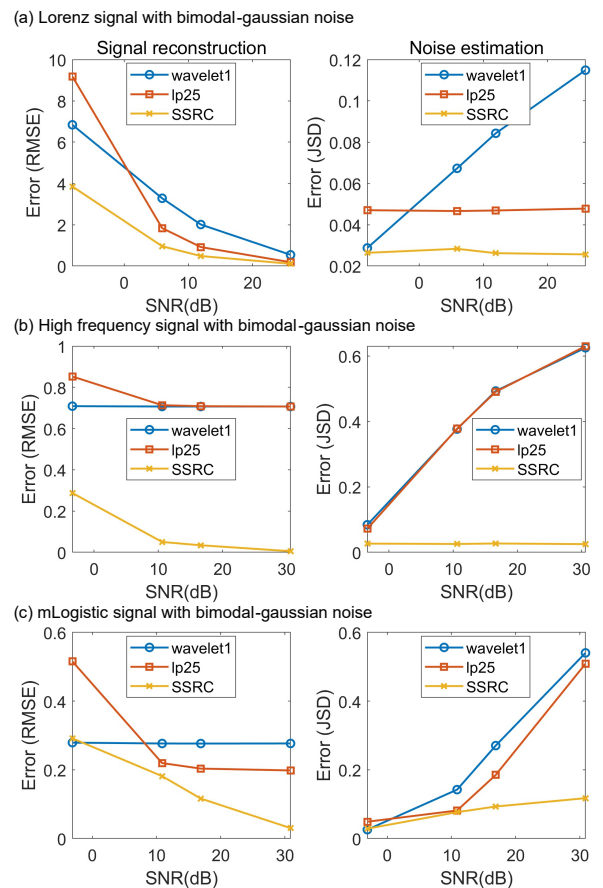


FIG. 7: Comparison of separation performance for bimodal noise according to SNR. (a) Lorenz signal corrupted by additive bimodal noise (b) Highly oscillating signal corrupted by additive bimodal noise

VIII. DISCUSSION

The method operates without prior knowledge of noise characteristics and effectively isolates deterministic signals

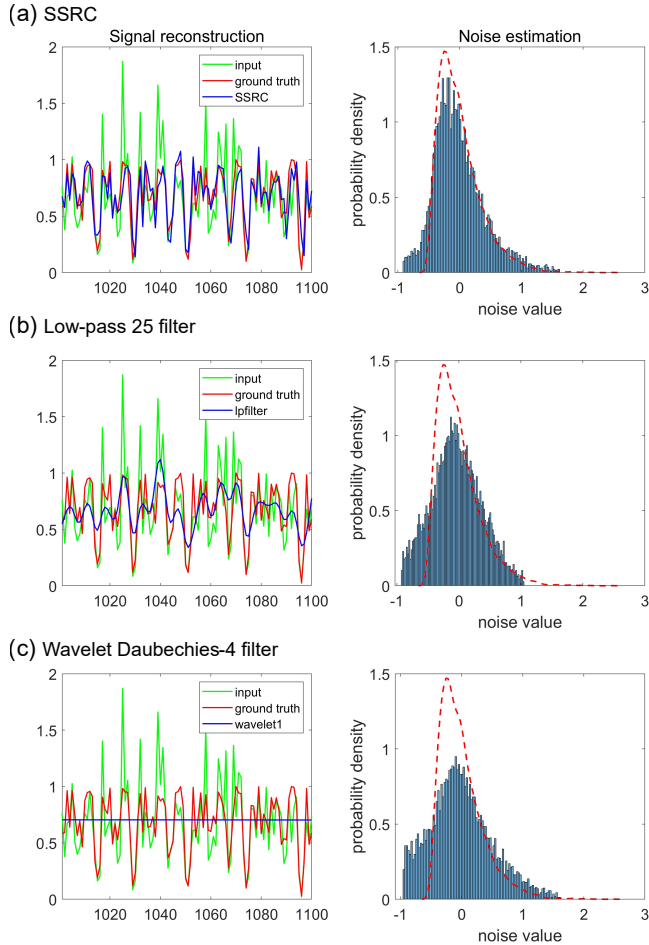


FIG. 8: (Color online) mLogistic signals x_i corrupted by multiplicative gamma noise with SNR=9(dB), (a) separation results of SSRC, (b) low pass filtering, (c) wavelet based filtering

from noise with diverse non-Gaussian distributions, encompassing symmetric and multimodal forms. Its efficacy has been validated across a range of signal and noise combinations, including chaotic signals contaminated with multiplicative gamma noise and highly oscillatory sinusoidal signals corrupted by intense additive noise.

The proposed method is flexible and simple, and at its core it exploits the ability of machine learning to maximize the extraction of deterministic patterns. The effect of noise is neutralized in the process of finding patterns in the signal, and then its distribution is recovered by comparing the restored pattern back to the original time series. The method can be considered as unsupervised learning in the sense that the predictor requires only single time series, the one that is subject to filtering. We used RC in this paper as a predictor, but there is no intrinsic difference in using any other popular predictors such as multi-layer perceptron or LSTM.

To avoid overfitting, we left a portion of the given signal as a validation set and used it to optimize the predictor's performance. The capacity of the predictor determined in this way

	Lorenz	High frequency	mLogistic
SSRC	0.2867	0.0670	0.1920
Wavelet1	0.6371	1.0001	0.3788
Wavelet2	0.6337	1.0001	0.3780
Low-pass Filtering25	0.6205	1.0129	0.3159
Low-pass Filtering50	0.8883	1.0263	0.2828
Low-pass Filtering75	1.1218	1.0415	0.3118
Median Filtering	0.7114	0.3224	0.3339
Adaptive filtering	0.3031	1.0026	0.3848

TABLE III: Mean reconstruction errors for multiplicative gamma noise with various data types of SNR values of -2.68 dB, 9 dB, and 9 dB for Lorenz, high-frequency, and mLogistic system, respectively, out of 100 realizations.

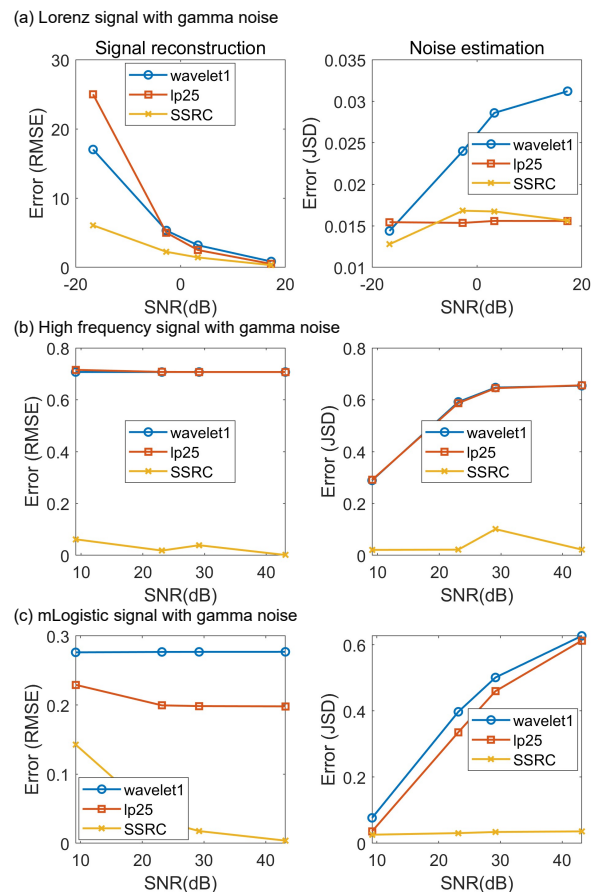


FIG. 9: Comparison of separation performance for multiplicative gamma noise according to SNR. (a) Lorenz signal (b) highly oscillating sinusoidal signals. In the right panels of each figure, the multiplicative noise distribution is estimated by the equation $\hat{\xi}_i = \psi_i/q_i$, and compared to the true one in JSD. In such estimation, 1% of q_i with the smallest magnitude is discarded to avoid potential overflow.

allows us to indirectly estimate SNR of the signal. In other words, the optimal capacity of the predictor, like the node

number of the reservoir, can be regarded as an indirect measure of the amount of deterministic information in the signal.

This paper mainly focused on separation of signals with additive and multiplicative noise. However, in practice, the signals are often corrupted by combination of those two types of error together. Separation of such noise requires more refined applications of time series prediction and will be studied in the future work.

Methods

All computations were carried out using MATLAB R2023a version. The simulation of the data system was conducted using the RK4 (Runge-Kutta 4th order method). Low-pass filtering, wavelet-based filtering, and Bayesian optimization were all implemented using MATLAB's built-in functions. Detailed explanations about parameter settings and the system equation can be found in the supplementary material.

Data availability

The authors declare that the data supporting the findings of this study can be recreated as described in the manuscript and also obtainable from the corresponding author upon request.

Acknowledgements

Author contributions

J.C. and P.K. conceived of the presented idea. J.C. developed the theory and performed the computations. P.K. supervised the project and wrote the manuscript.k

Competing interests

Authors declare no competing interests.

Correspondence and requests for materials should be addressed to Pilwon Kim.

References

- ¹H. Attias and C. E. Schreiner, "Blind source separation and deconvolution: the dynamic component analysis algorithm," *Neural computation*, vol. 10, no. 6, pp. 1373–1424, 1998.
- ²E. Moulines, J.-F. Cardoso, and E. Gassiat, "Maximum likelihood for blind separation and deconvolution of noisy signals using mixture models," in *1997 IEEE international conference on acoustics, speech, and signal processing*, vol. 5. IEEE, 1997, pp. 3617–3620.
- ³D. Kundur and D. Hatzinakos, "Blind image deconvolution," *IEEE signal processing magazine*, vol. 13, no. 3, pp. 43–64, 1996.
- ⁴P. Campisi and K. Egiazarian, *Blind image deconvolution: theory and applications*. CRC press, 2017.
- ⁵N. Borodinov, S. Neumayer, S. V. Kalinin, O. S. Ovchinnikova, R. K. Vasudevan, and S. Jesse, "Deep neural networks for understanding noisy data applied to physical property extraction in scanning probe microscopy," *npi Computational Materials*, vol. 5, no. 1, p. 25, 2019.
- ⁶Y. Li, Z. Li, K. Wei, W. Xiong, J. Yu, and B. Qi, "Noise estimation for image sensor based on local entropy and median absolute deviation," *Sensors*, vol. 19, no. 2, p. 339, 2019.
- ⁷M. Coulon, J.-Y. Tournet, and A. Swami, "Detection of multiplicative noise in stationary random processes using second-and higher order statistics," *IEEE transactions on signal processing*, vol. 48, no. 9, pp. 2566–2575, 2000.
- ⁸T. S. Uhm et al., "Multiplicative noise model and composite signal detection," in *IEE Proceedings F (Radar and Signal Processing)*, vol. 138, no. 6. IET, 1991, pp. 531–538.
- ⁹B. Schrauwen, D. Verstraeten, and J. Van Campenhout, "An overview of reservoir computing: theory, applications and implementations," in *Proceedings of the 15th european symposium on artificial neural networks*, p. 471-482 2007, 2007, pp. 471–482.
- ¹⁰H. Jaeger, "The "echo state" approach to analysing and training recurrent neural networks-with an erratum note," Bonn, Germany: German National Research Center for Information Technology GMD Technical Report, vol. 148, no. 34, p. 13, 2001.
- ¹¹H. Jaeger and H. Haas, "Harnessing nonlinearity: Predicting chaotic systems and saving energy in wireless communication," *science*, vol. 304, no. 5667, pp. 78–80, 2004.
- ¹²J. Gao, H. Sultan, J. Hu, and W.-W. Tung, "Denoising nonlinear time series by adaptive filtering and wavelet shrinkage: a comparison," *IEEE signal processing letters*, vol. 17, no. 3, pp. 237–240, 2009.
- ¹³F. Wang and V. Balakrishnan, "Robust kalman filters for linear time-varying systems with stochastic parametric uncertainties," *IEEE transactions on signal processing*, vol. 50, no. 4, pp. 803–813, 2002.
- ¹⁴E. Todorov and M. I. Jordan, "Optimal feedback control as a theory of motor coordination," *Nature neuroscience*, vol. 5, no. 11, pp. 1226–1235, 2002.
- ¹⁵C. M. Harris and D. M. Wolpert, "Signal-dependent noise determines motor planning," *Nature*, vol. 394, no. 6695, pp. 780–784, 1998.
- ¹⁶R. F. Fox and R. Roy, "Steady-state analysis of strongly colored multiplicative noise in a dye laser," *Physical Review A*, vol. 35, no. 4, p. 1838, 1987.